PROCEEDINGS, 47th Workshop on Geothermal Reservoir Engineering
Stanford University, Stanford, California, February 7-9, 2022
SGP-TR-223

Performance of Hydroxyapatite Containing Cement in HPHT Acidic Environments

Ramadan Ahmed, Saeed Salehi, and Aman[1] Srivastava

Mewbourne School of Petroleum and Geological Engineering, University of Oklahoma, Norman, OK, USA

r.ahmed@ou.edu

Keywords: Cement; Degradation: Carbonic acid; Hydroxyapatite: Carbonation

ABSTRACT

The working fluid in geothermal wells often contains naturally occurring CO_2. In an aqueous environment, CO_2 forms carbonic acid and subsequently reacts with the binding components of cement, resulting in the loss of strength and early failure. Well cement formulations containing hydroxyapatite (HOAP) are considered resistant to the carbonic acid attack. The main goal of this work is to study the effects of hydroxyapatite on cement degradation in high-pressure, high-temperature (HPHT) acidic environments.

For evaluating the performance of HOAP cement, aging experiments were conducted using cement cores and shear-bond test specimens. The aging temperature, pressure, and CO_2 content of the gas were varied. After aging, the cores and specimens were recovered and tested to assess the level of degradation based on variation in bond and compressive strengths, porosity, permeability, and mineralogical composition.

The results showed that HOAP cement has better resistance to carbonic acid attack than the baseline cement that does not contain hydroxyapatite. Nevertheless, due to the lack of silica flour, HOAP samples were thermally degraded after aging under extremely harsh conditions and exhibited high permeability due to the formation of microcracks.

1. INTRODUCTION

Calcium hydroxyapatite (also known as hydroxyapatite) occurs naturally like other minerals. It is regularly used in orthopedic and dental applications because of its biocompatibility and osteoconductivity (Teraoka et al. 1998). Studies on cement containing hydroxyapatite are limited. This type of cement exhibits increased resistance to carbonic acid (Sugama 2006; Sugama and Carciello 1992; 1993). It was used in various geothermal wells, including in Indonesia, Japan, and the USA. The significant advantage of the cement is the saving of repair cost (Sugama 2006). Despite its resistance to carbonic acid attack by creating a protective layer, hydroxyapatite-based cement has lower compressive strength than neat cement containing no hydroxyapatite (Sugama and Carciello 1992; Martin and Brown 1995).

When well cement is placed in the wellbore, it can be exposed to the formation fluid containing brine saturated with CO_2. Hydration and solidification occur in the wellbore under harsh conditions. The hydration process produces the cement's main binding components (calcium hydroxide and calcium silicate hydrate). These binding materials can react with carbonic acid and form $CaCO_3$ crystals in the pore space (Brandl et al. 2010). The formation of these crystals reduces cement porosity and permeability. Gradually, the produced calcium carbonate reacts with excess carbonic acid and forms calcium bicarbonate, which is highly water-soluble. Consequently, the calcium bicarbonate can be leached out with the surrounding fluid. The loss of calcium hydroxide (CH) and calcium silicate hydrates (CSH) occurs in two steps (i.e., carbonation followed by the bicarbonation process), resulting in rapid loss of strength and sealing performance due to increased porosity and permeability. The change in the essential properties of cement indicates the level of degradation. Because of the involvement of various chemical and physical mechanisms, environmental factors such as temperature, pressure, the composition of the surrounding fluid, and its pH strongly influence the degradation process.

2. CEMENT DEGRADATION

Under HPHT acidic environment, cement degradation could occur in different forms i) chemical degradation such as carbonation, ii) direct leaching of binding components surrounding fluid, and iii) property change due to phase transformation.

2.1 CARBONATION

Cement degradation happening under downhole conditions comprises several physicochemical processes, including i) the transport of ions in a porous medium; ii) chemical reactions between CH, CSH, and calcium carbonate and carbonic acid (i.e. carbonation and bicarbonation processes), and iii) dissolution and leaching of the binding components and bicarbonation products.

Carbon dioxide is water-soluble gas that dissolves in water, forming carbonic acid that penetrates the cement matrix and attacks the main binding components (CH and CSH). The attack leads to cement degradation, which involves a series of physicochemical processes,

[1] Currently with Halliburton-Landmark

including carbonation, bi-carbonation, and leaching of the binding components of hydrated cement. The chemical reaction steps are often summarized as (Santra and Sweatman 2011; Benge 2009; Duguid 2009; Kutchko et al. 2007; Gerard et al. 2002):

$$CO_2 + H_2O \rightarrow H_2CO_3 \quad (1)$$

$$H_2CO_3 + CH/CSH \rightarrow CaCO_3 + \text{Silica Gel} \quad (2)$$

$$H_2CO_3 + CaCO_3 \rightarrow Ca(HCO_3)_2 \quad (3)$$

According to these reaction steps, CO_2 dissolves in the surrounding aqueous medium and form carbonic acid, which can react with the binding components of the cement. The acid penetrates the cement matrix and reacts with its binding components, resulting in the formation of $CaCO_3$ crystals that precipitate in the available cement pore space. The precipitation reduces the porosity and permeability of the cement. The cement density is expected to increase after carbonation because of the packing of the pores with the crystals (Bjørge et al. 2019; Šavija and Luković 2016). The reduction in porosity and permeability restricts further penetration of carbonic acid. The packing of the pores also expands the cement and improves its compressive and shear bond strengths.

Although these property changes, which occur in the early stage of the degradation, appear to be favorable to cement, in the presence of carbonic acid, bi-carbonation of $CaCO_3$ happens when the pH is less than 11. The product of bi-carbonation is $Ca(HCO_3)_2$, which is highly soluble in water. Therefore, $Ca(HCO3)_2$ can be extracted from the cement matrix, causing an increase in porosity and permeability (Bjørge et al. 2019; Santra and Sweatman 2011; Kutchko et al. 2007). The extraction of bi-carbonates (leaching) is accompanied by the unpacking of the pores, reducing the compressive and shear-bond strengths of cement and increasing its porosity and permeability. The increase in porosity and permeability promotes further acid attack and facilitates the leaching process. In hydroxyapatite-containing cement, carbonic acid not only reacts with the primary binding components but also reacts with calcium hydroxyapatite ($Ca_5(PO_4)_3(OH)$). Then, it forms carbonated hydroxyapatite ($Ca_5(PO_4)_3CO_3$) as shown in the following reaction equation:

$$2Ca_5(PO_4)_3(OH) + CO_3^{-2} \rightarrow 2Ca_5(PO_4)_3(CO_3) + 2OH^- \quad (4)$$

Like hydroxyapatite, the carbonated-hydroxyapatite exhibits hexagonal crystal structure, and its solubility in water is limited. As a result, it creates a stable, protective layer around the cement sheath that limits the acid penetration and carbonation of the primary binding components (Sugama 2006). **Figure 1** presents the expected cement properties and mineralogical composition trends in the carbonic acid environment. XHO and XS represent cement formulations with and without hydroxyapatite, respectively.

The degradation process is classified into three phases (penetration phase, carbonation phase, and bi-carbonation phase). In the penetration phase (Phase I), the acid penetrates the cement matrix with time. In this phase, cement property and composition changes are expected to the minimum. The acid penetration is followed by the carbonation phase (Phase II). Because of the carbonation, cement porosity and permeability decrease with time as the cement cores are being packed with calcium carbonates crystals. The packing improves the compressive and shear bond strengths of the cement. The CH and CSH contents of the cement also decrease with time due to the consumption of these components by the carbonation reaction, which produces calcium carbonate as the main reaction product. As a result, the calcium carbonate content of the cement increases with time in the carbonation phase. In the presence of excess carbonic acid, the bi-carbonation phase (Phase III) occurs. In this phase, carbonic acidic reacts with calcium carbonate crystals and produces calcium bicarbonate which is readily soluble in the surrounding fluids (Krilov et al. 2000). The removal of the crystals increases the porosity and permeability of the cement and decreases it's compressive and shear bond strengths.

Moreover, the bi-carbonation process occurring in Phase III reduces the calcium carbonate contents of the cement. Therefore, the property changes are expected to be more pronounced with cement formulation that doesn't contain hydroxyapatite (XS). The introduction of hydroxyapatite in the cement is expected to slightly decrease the initial cement compressive and shear bond strengths (Sugama 2006).

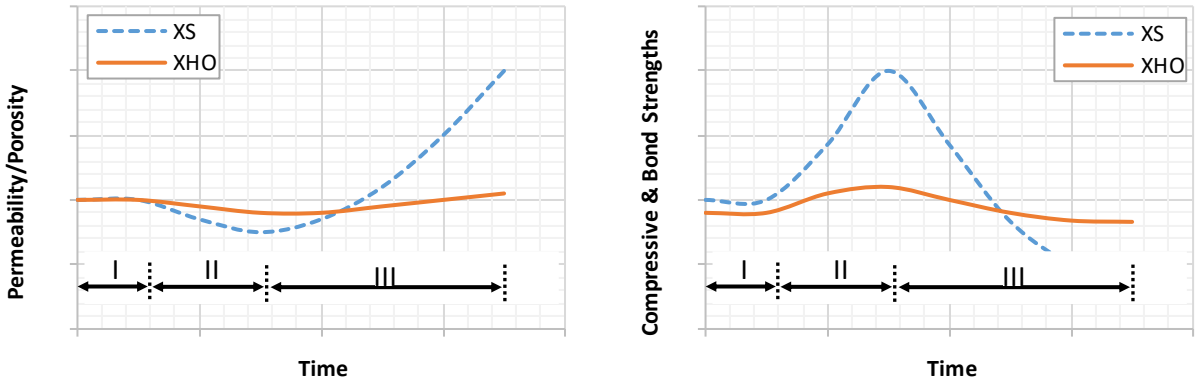

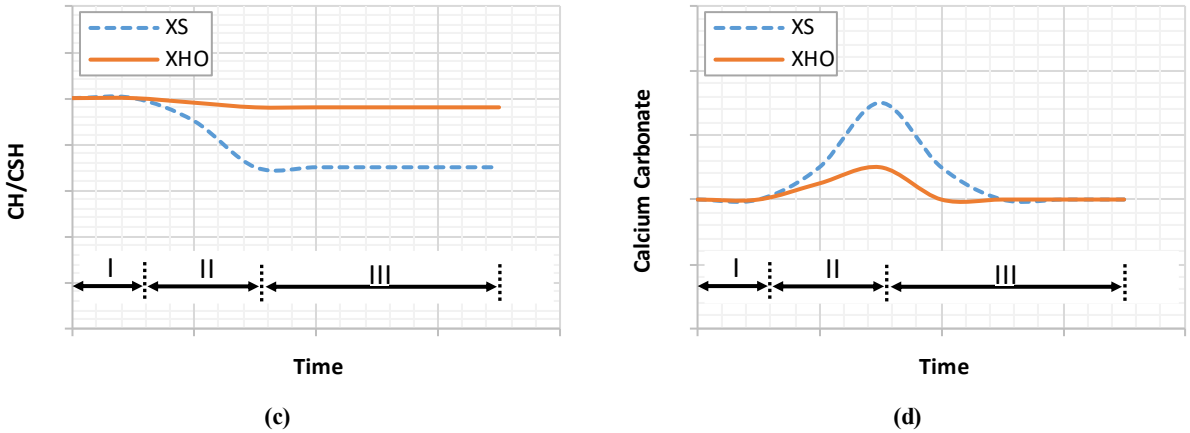

Fig. 1: Anticipated trends of cement characteristics with time: a) porosity, b) permeability, c) CH/CSH content, and d) calcium carbonate contents

2.2 DISSOLUTION AND LEACHING

Another mechanism of cement degradation is direct dissolution and leaching of the binding components (CH and CSH). Even though the direct leaching rate is usually low, this type of degradation is challenging to control as it depends on several factors, including the components' solubility, which is a function of temperature, solution pH, and the composition of formation fluid. Neglecting the effect of coexisting ions such as sodium and potassium ions, the solubility product of CH (Ksp) in sodium chloride solution is a function of temperature and chloride ion concentration (Nakarai et al. 2006). Thus:

$$Ksp = Ksp^{T} + Ksp^{Cl} \tag{5}$$

where Ksp^{T} and Ksp^{Cl} are solubility product functions which account for temperature and chloride concentration effects on the solubility of CH. The solubility product function that accounts for temperature on CH solubility is given as:

$$Ksp^{T} = 1.25 \times 10^{11} \times e^{-0.019T} \tag{6}$$

The solubility product function that accounts for chloride ion concentration on CH solubility is given as:

$$Ksp^{Cl} = A(5 \times 10\text{-}4\ ) \times (X_{NaCl})^{1/3} \tag{7}$$

A is an empirical parameter that varies with the concentration of sodium chloride. According to Eqn. (7), the solubility of CH reduces with temperature. The reduction in the solubility of CH is an important observation even though other forms of cement degradation could be substantial.

After hydration, the cement pores are filled with the formation brine and saturated with calcium ions (C_{satu}), while the surrounding bulk fluid has a negligible concentration of calcium ions. This causes ionic diffusion towards the bulk fluid. The diffusion process depends upon several factors such as porosity, permeability, and temperature. Due to the diffusion of calcium ions from the pore fluid to the bulk, de-saturation of the calcium ions occurs, leading to the dissolution of CH or CSH from the matrix. Hence, a leaching front is generated in the matrix, which slowly progresses ahead. The physical effects of leaching are increases in porosity and permeability and reductions in compressive and shear bond strengths. The solubility of calcium from CH is higher than CSH (Nakarai et al. 2006); however, the solubility product of CSH varies with the CaO/SiO_2 ratio of the cement.

2.3 Phase Transformation

The phenomenon of thermal retrogression is a possible form of cement degradation at high temperatures. Cement composition determines how the temperature influences its property, most importantly, the calcium to silica ratio. At high calcium to silica ratios (CaO/SiO_2 greater than 1.0), the tobermorite phase (CSH) converts into a less stable dicalcium silicate hydrate (a-C_2SH phase) when the temperature is more than 110°C. The conversion results in reduced cement compressive strength and increased permeability. Adding silica flour to the cement prevents the transformation and allows the formation of CSH, which is more stable than a-C_2SH. However, at higher temperatures (greater than 150°C), the tobermorite converts into xonotlite and/or gyrolite (Taylor 1964; Omosebi et al 2016; 2017). Xonotlite is a more stable and robust form of CSH phase with moderate permeability. At extremely high temperatures (greater than 215°C), weak and less permeable truscottite phase forms and reduces the compressive strength of cement. Even though temperature and cement composition primarily affect the transformation process, other factors such as the ionic composition of pore fluids can influence the conversion of CSH.

2.4 Effect of Environmental Factors

1.2.1 Temperature

High reservoir temperature is a common characteristic of geothermal wells. The effect of temperature on cement carbonation is complex due to the involvement of contradictory mechanisms such as dissolution and transport of reactants and products in the pore and bulk fluid surrounding cement. Besides this, temperature influence the carbonation reaction kinetics. The solubility of the reactants, presented in Eqns. (1) and (2), strongly influenced by temperature. Increasing temperature lowers the solubility of CH and CSH (Bassett 1934; Glasser et al. 2005; Nakarai et al. 2006). Moreover, the solubility of CO_2 in the surrounding solution is influenced by temperature and pressure (**Fig. 2**). Usually, the solubility of gases at a given pressure decreases with temperature. However, carbon dioxide displays (Duan and Sun 2003) abnormal solubility trend at high pressures and temperatures (i.e. greater than 20 MPa and 70°C).

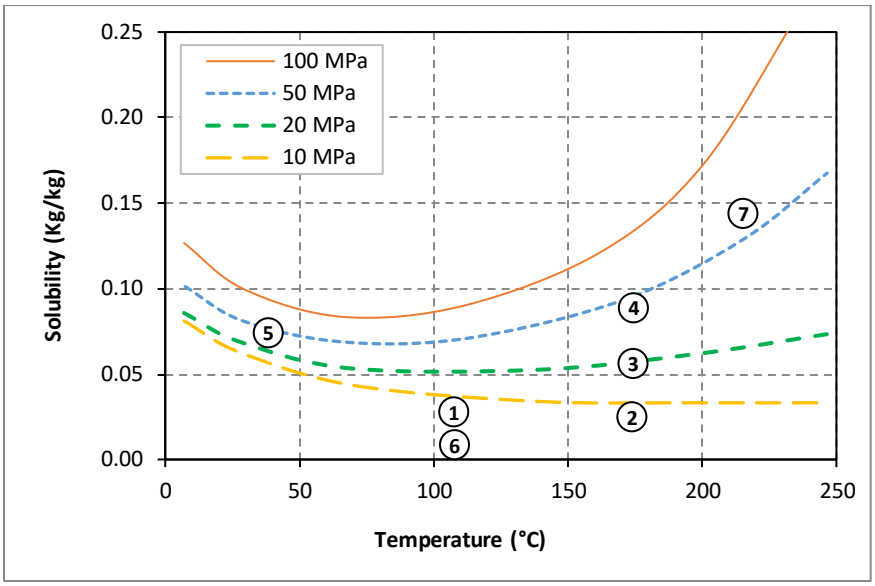

Fig. 2: Solubility of CO_2 in pure water and comparing experiments conducted at 100% CO_2 (Data from Duan and Sun 2003)

In addition to affecting the solubility of CO_2, temperature substantially influences the carbonation process. Several studies (Papadakis et al. 1991; Loo et al. 1994; Matsuzawa et al. 2010) investigated the effect of temperature on carbonation. In these studies, the level of carbonation was quantified using carbonation depth measurements as a function of time. Even though some discrepancies and uncertainties were observed, the general trend of the measurements indicates an increase of carbonation rate with temperature.

Temperature influences the transport process of reactant and product species (ions and molecules) that affect the carbonation process of cement. Molecular diffusion is the primary ionic transport mechanism in porous materials that temperature can facilitate. For instance, the diffusion coefficient of calcium ion in cement increased twofold when the temperature increased from 10 to 40°C (Samson. and Marchand 2007). The diffusion coefficient of other ions such as chloride, sodium, and potassium ions also increased similarly.

1.2.2 Pressure

In addition to temperature, pressure directly affects the solubility of CO_2 in aqueous solutions (Fig. 2). The solubility of carbon dioxide increases with pressure. The increase is more pronounced than at high temperatures (greater than 150°C). Hence, increasing pressure facilitates the dissolution of CO_2 and increases the reactant concentration and the carbonation reaction. Therefore, the amount of CO_2 dissolved in the surrounding solution determines CH and CSH's carbonation.

Glasser and Matschei (2007) showed the effects of the CO_2 content of cement on the carbonation process. The mineralogical changes occurring due to the carbonation along the penetration depth direction were strongly related to CO_2 concentration (**Fig. 3**). CH is more reactive to carbonic acid than CSH. As a result, CH carbonation occurred first and was followed by the carbonation of CSH. The results showed the presence of three cement carbonation zones: fully carbonated zone (Zone I), CSH carbonation zone (Zone II), and CH carbonation zone (Zone III). The concentration of CO_2 decreased with the penetration depth because of the carbonation reaction. The concentration of the reaction product (calcium carbonate) also decreased with the penetration depth due to the reduction in carbonic acid concentration and exposure time. In the carbonated zone, the concentrations of CH and CSH were negligible, and calcium carbonate concentration remained the same. In the CSH carbonation zone, CH was completely neutralized by the acid, whereas CSH was partially consumed. Therefore, the consumption of CSH decreased with the penetration depth in this zone. In the CH carbonation zone, CH was partially consumed. Thus, the CH consumption was reduced with the penetration depth.

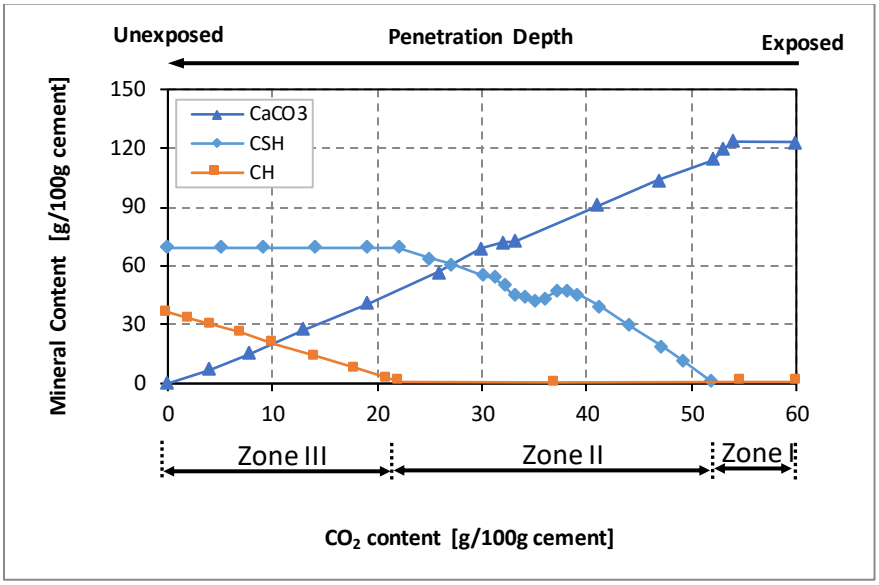

Fig. 3: Impact of carbonation on the mineralogical composition of hydrated model cement and CO_2 partial pressure of 35 Pa (Data from Glasser and Matschei 2007)

3. EXPERIMENTAL STUDY

3.1 Cement Formulations

Two classes of API cement (Class H and Class G) were used in this investigation. For both cement classes, slurry formulations were developed with and without hydroxyapatite. Cement formulations without hydroxyapatite were used as baselines for evaluating the benefit of hydroxyapatite. Hydroxyapatite containing (HOAP) cement formulations (HHO and GHO) were adjusted to maintain similar slurry properties between baselines and HOAP formulations. HOAP cement slurries showed excessive thickening; as a result, HEC and silica flour were removed from these formulations (**Table 1**). In addition, citric acid was introduced to the HOAP cement formulations to reduce the slurry viscosity and increase the thickening time. Silica flour is not required when hydroxyapatite is used as the primary cement component. The exclusion of silica is because hydroxyapatite is considered resistant to thermal retrogression (Sugama 2006). Therefore, the HOAP formulations were prepared without silica flour. However, the silica flour was added to the baseline formulations to maintain their CaO/SiO_2 ratio below 1.0. High temperature with cementing, silica flour is normally added to prevent the thermal retrogression of tobermorite phase (Dillenbeck et al. 1990; Eilers et al. 1983; Eilers and Root 1976; Grabowski and Gillott 1989; Lea 1971).

Table 1: Slurry compositions

Component	Baseline Class H (HS)	HOAP Class H (HHO)	Baseline Class G (GS)	HOAP Class G (GHO)
Class H cement	100%	100%	100%	100%
Silica flour	35% bwoc	-	35% bwoc	-
Fluid loss additive (HEC)	0.1% of water for silica flour	-	0.1% of water for silica flour	-
Anti-foaming agent	0.38 L/sk of cement	0.38 L/sk of cement	0.38 L/sk of cement	0.38 L/sk of cement
Water for cement	38% bwoc	38% bwoc	44% bwoc	44% bwoc
Water for silica flour	38.5% of silica flour	38.5% of silica flour	38.5% of silica flour	38.5% of silica flour
Citric Acid	-	0.125% bwoc	-	0.125% bwoc
hydroxyapatite	-	5% bwoc	-	5% bwoc
Water for hydroxyapatite	-	23% by weight of hydroxyapatite	-	23% by weight of hydroxyapatite

3.2 Slurry Properties

The baseline and HOAP slurries were prepared as per the API procedure (RP10B 1997). Relevant cement properties presented in **Table 2** were measured (density, rheology, filtration loss, and thickening time) after the preparation of the cement slurries. The rheological behaviors of the slurries are represented by the power-law model ($\tau = k\dot{\gamma}^n$). The flow curves of HOAP slurries were between those of baseline cement (Class H and Class G) slurries, indicating acceptable fluidity. In addition, the calculated and measured densities of the slurries were approximately the same.

Table 2: Properties of HOAP and baseline cement slurries

Property		Unit	HHO	HS	GHO	GS
Theoretical Density		g/cm^3	8.20	7.98	7.89	7.76
Measured Density		g/cm^3	8.20	8.10	7.85	7.73
Filtrate volume at 7.5 min.		ml	67	50	65	60
Rheological Parameters	n	-	0.31	0.44	0.34	0.35
	k	Pas^n	10.3	6.9	9.7	5.0
Thickening Time		min	165	170	130	135

3.3 Preparation of Cement Cores and SBS Samples

After preparation, baseline and HOAP cement slurries were poured into rubber molds and immersed in a vessel containing brine (2% NaCl solution). The vessel was sealed and placed in a temperature-controlled oven for curing. Concurrently, specimens used to measure shear bond strength (SBS) were prepared by pouring the slurry into short pieces of steel pipes with a length of 4.45 cm and an internal diameter of 1.88 cm. The pipes' external surface was coated with high-temperature resistant paint to prevent corrosion; and they were plugged on one end with a short piece (1-cm long) of rubber cork. The slurry was carefully poured into the pipes, and the specimens were placed in a vessel containing brine. The details of the SBS specimen preparation are presented elsewhere (Hwang et al. 2018; Srivastava et al. 2019). Next, the vessel was placed in an oven for curing. The curing was for five days at 93°C for cement samples and SBS specimens. After curing, the hardened cement samples were recovered from the oven, and 2.54-cm cylindrical cores with a length of 3.81 cm were cut from the samples. SBS specimens were also recovered after curing.

3.4 Aging Conditions

After preparing SBS specimens and cement cores, aging was performed in brine (2% NaCl solution) for two weeks, saturated with mixed gas containing CO_2 and CH_4. To assess the benefits of hydroxyapatite, seven aging experiments (**Table 3**) were conducted varying the test pressure, temperature, and CO_2 content that is defined as the ratio of CO_2 partial pressure to the total pressure. Experimental conditions are shown in Fig. 2 to estimate the solubility of CO_2 under the aging condition (i.e., using temperature and partial pressure of CO_2). To evaluate the influence of aging, half of the SBS specimens and cement cores were kept in brine under ambient conditions without exposure to acidic gas.

Table 3: Aging conditions for the experiments

Test Parameters	Exp. 1	Exp. 2	Exp. 3	Exp. 4	Exp. 5	Exp. 6	Exp. 7
Temperature	107°C	177°C	177°C	177°C	38°C	107°C	221°C
Total Pressure	21 MPa	21 MPa	21 MPa	42 MPa	42 MPa	21 MPa	63 MPa
CO_2 content	40 %	40 %	100 %	100 %	100 %	10 %	100 %
Partial pressure of CO_2	8.4	8.4	21	42	42	2.1	63
Baseline samples	HS* & GS	HS* & GS	HS* & GS	HS* & GS	HS* & GS	HS* & GS	HS* & GS
HOAP samples	HHO* & GHO	HHO* & GHO	HHO* & GHO	HHO* & GHO	HHO* & GHO	HHO* & GHO	HHO* & GHO

* Data presented in a previous study (Srivastava et al. 2019)

3.5 Aging Setup and Procedure

Figure 4 shows the schematic of the aging setup. The setup consists of: i) aging cell/autoclave; ii) two gas supply cylinders; iii) gas injection system; iv) autoclave heating system; and v) measuring and data acquisition (DAQ) system. The autoclave is a jacketed vessel with a volumetric capacity of 3 L. The function of the injection system is to measure and pressurize the supply gas required for the aging process. The SBS specimens and cement cores were arranged on a cylindrical shelf/rack with perforations during aging. After the arrangement, the rack was carefully positioned in the autoclave. The cell was then filled with brine until all samples and cores were entirely immersed in the brine. Subsequently, the cell was sealed by placing the lid and connected to the gas inlet line. Next, the autoclave was heated by circulating the heating medium through its jacket. The gas injection was started when the desired cell temperature was reached. The injection was continued until the desired cell pressure was achieved. Then, experimental parameters were maintained

constant for two weeks. When the aging was completed, the cell was slowly depressurized, and the specimens and cores were recovered. The experimental setup and test procedure details are presented elsewhere (Ahmed et al. 2015; Omosebi et al. 2015; 2016).

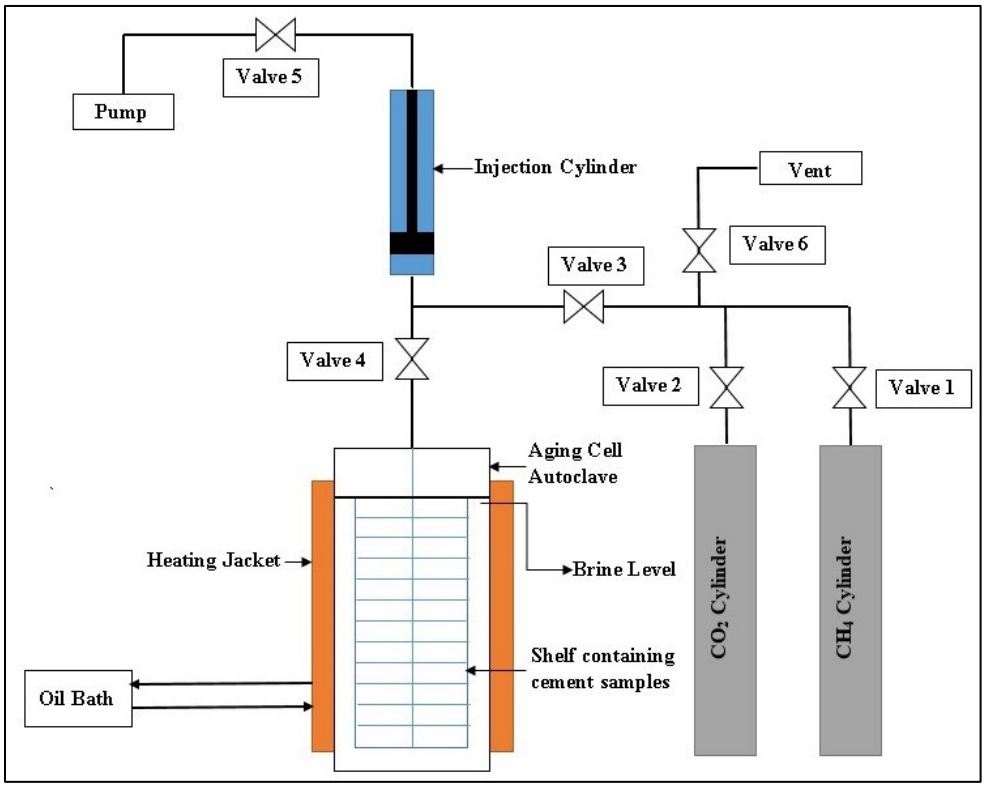

Fig. 4: Aging setup (Srivastava 2014)

3.6 Degradation Assessment Methods

The physical and mechanical properties (porosity, permeability, and compressive strength) and mineralogical compositions of HOAP cement cores were measured and compared with that of the baseline cement to evaluate the benefits of HOAP cement. An automated gas porosity-permeability meter (Coretest Model AP-608) was used to measure the porosity and permeability of dried cement cores.

The compressive strength of the cores was measured using a custom-made triaxial compression machine with a Hassler sleeve-type core holder. The confining pressure was maintained at 6.9 MPa while an increasing axial load was gradually applied according to ASTM-C39/C39M-12 standard. The resulting stress in the cement was measured as a function of time until the material exhibited a failure. The SBS of the specimens was also measured using specially-made equipment developed for measuring SBS (Ahmed et al. 2015). The equipment gradually applies an axial force on the cement from inside while firmly holding the specimen. The force was applied until the bond between the pipe in the cement broke. The maximum force is used to determine the SBS.

Dried cement cores used for measuring porosity and permeability were cut transversely to collect samples for the Fourier-transform infrared spectroscopy (FTIR) test. Cement samples were collected at three locations in the radial direction i) core center, ii) core wall, and iii) mid-point. Conventional FTIR equipment (Thermo Scientific, Model Nicolet 6700) was utilized to perform the FTIR tests.

4. RESULTS AND DISCUSSION

The advantage of using hydroxyapatite as a cement additive to delay the carbonation of its primary binding components was assessed by comparing property changes occurring after exposure to HPHT carbonic environment. The properties selected for this evaluation are porosity, permeability, compressive strengths, and mineralogical composition.

4.1 Porosity

Zonal isolation and structural support are the primary functions of well cement. Therefore, porosity is one of the critical properties of cement that determines its sealing performance. **Figure 5** compares the porosity of hydroxyapatite-based (HOAP) cements with that of their corresponding baselines (HS and GS). The porosity of baseline samples consistently decreased after aging due to the carbonation of CH and CSH and the formation of calcium carbonate crystals in the pore space. The HOAP samples demonstrated mixed results. In Experiments 1, 2, and 3, the porosity of HHO samples slightly increased after aging, indicating the absence of noticeable carbonation. However, in other experiments, HHO samples demonstrated some reduction in porosity. Overall, the average porosity of the HHO samples reduced by 18% while that of the baseline samples (HS) decreased by 47%, indicating a greater level of carbonation than the HS samples (**Fig. 6**). Similarly, the porosity of GHO samples increased after aging in two cases (Experiments 1 and 3), whereas the baseline samples consistently showed porosity reduction. In this case, the difference between the average porosity reductions of GHO and GS samples is

about 10%. This slight difference is mainly because Class H cement was more susceptible to carbonation than Class G cement. As a result, the impact of using hydroxyapatite was more pronounced in the case of Class H cement.

Even though the general observation is consistent with carbonation and the expected impact of hydroxyapatite, some cases are unexpected or require explanations. For instance, the baseline samples showed an extreme reduction in porosity after aging at 177°C, 21 MPa, and 40% CO_2 (Experiment 2). This reduction is unexpected considering low CO_2 solubility (Fig. 2) resulting from low total pressure and reduced CO_2 content. Furthermore, in Experiment 7, the HHO samples demonstrated the highest reduction in porosity when aged under high pressure and high-temperature condition (63 MPa and 221°C). Possible explanations for this observation could be rapid diffusion and increased solubility of CO_2. High temperature caused rapid diffusion of carbonate ions into the cement pore resulting in carbonation of the matrix. Moreover, the HPHT condition increased CO_2 solubility (Fig. 2) and facilitated the carbonation process resulting in severe reduction in the porosity of the samples.

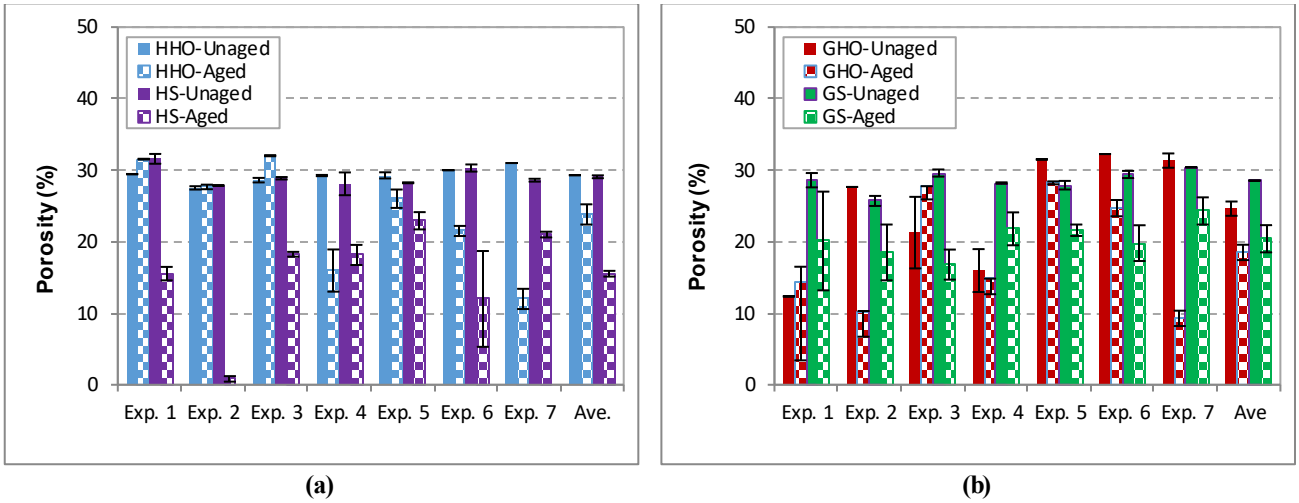

Fig. 5: Porosity of HOAP and baseline samples: a) HHO and HS, and b) GHO and GS

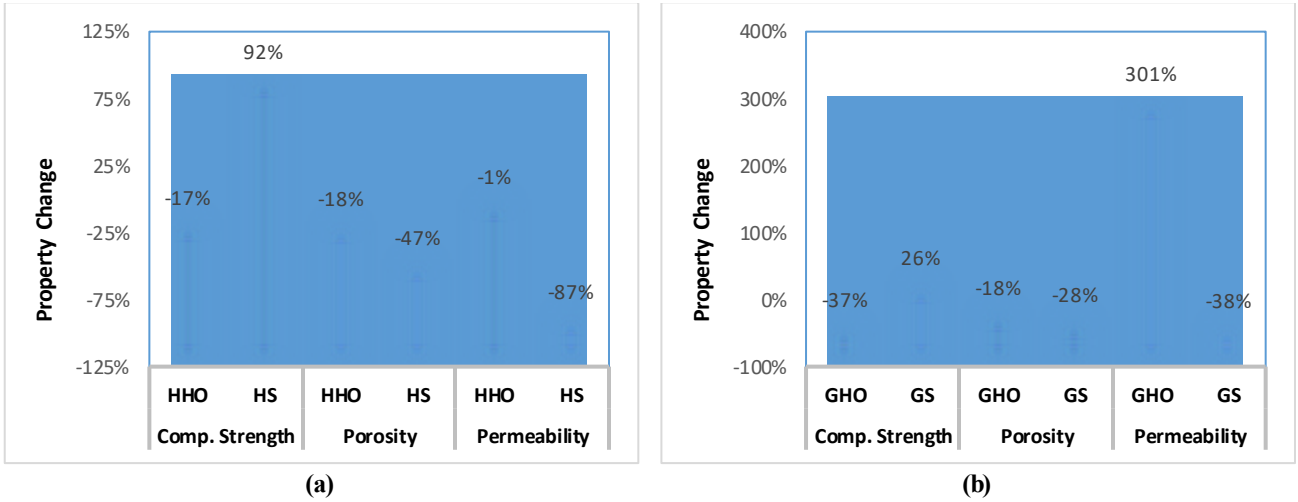

Fig. 6: Average property change after aging: a) HHO and HS, and b) GHO and GS

4.2 Permeability

The permeability of HOAP and baseline samples significantly changes after aging (**Fig. 7**). The charts are presented as logarithmic plots for better visualization. Except for one case (Experiment 4 with GS samples), baseline samples exhibited a reduction in their permeability. The reduction is consistent with the porosity decline observed after aging due to carbonation of CH and CSH. The extreme decline in the permeability of baseline samples demonstrated severe carbonation of the cement resulting in the formation of calcium carbonate crystals in the pore space. The formation of the crystals around the pore throat can cause a severe reduction in permeability. In contrast, HOAP samples exhibited both an increase and a decrease in permeability. As a result, the average permeability of the HOAP samples increased after aging even though that of the baseline showed a noticeable decline. The HOAP samples demonstrated better resistance for carbonation than the baseline samples.

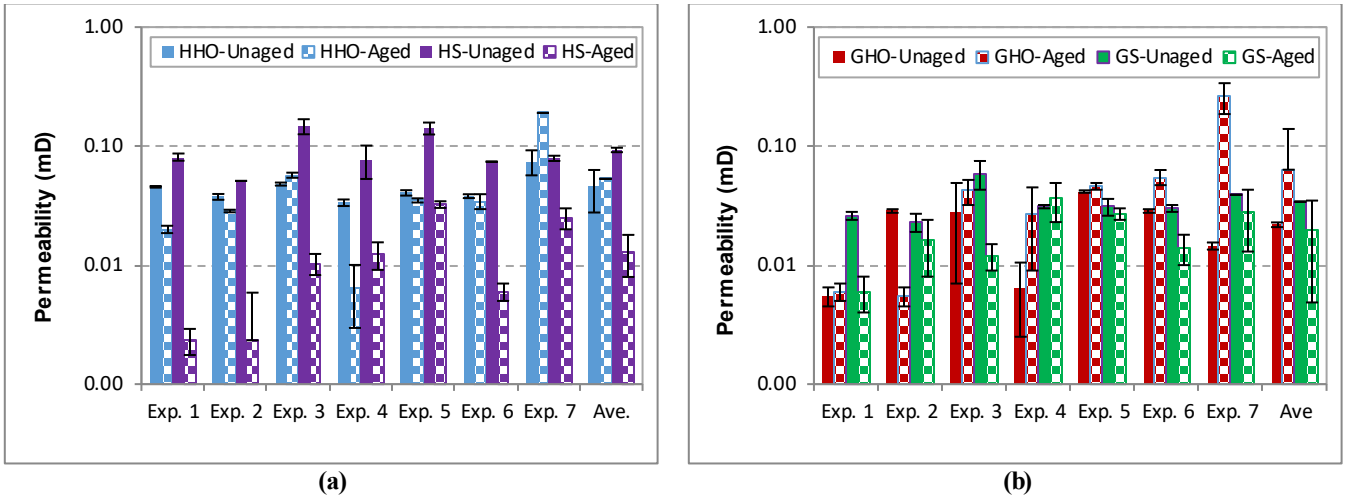

Fig. 7: permeability of HOAP and baseline samples: a) HHO and HS, and b) GHO and GS

Contrary to the severe porosity reduction observed, the permeability of HOAP samples increased substantially (up to tenfold) after aging at HPHT condition (Experiment 7). These unexpected results can be explained by considering the impact of thermal retrogression on the property of cement. Due to the lack of silica flour, thermal retrogression could be more severe for HOAP samples than the baselines. Furthermore, when the temperature is above 215°C, CSH transforms to the truscottite phase, which is weak and could be more susceptible to developing microcracks that can increase the permeability of cement. HOAP cores that were cross-section after aging (**Fig. 8**) exhibited microcracks which were not present in the baseline samples. As a result, the HOAP samples exhibited an extremely high increase in permeability than the baselines.

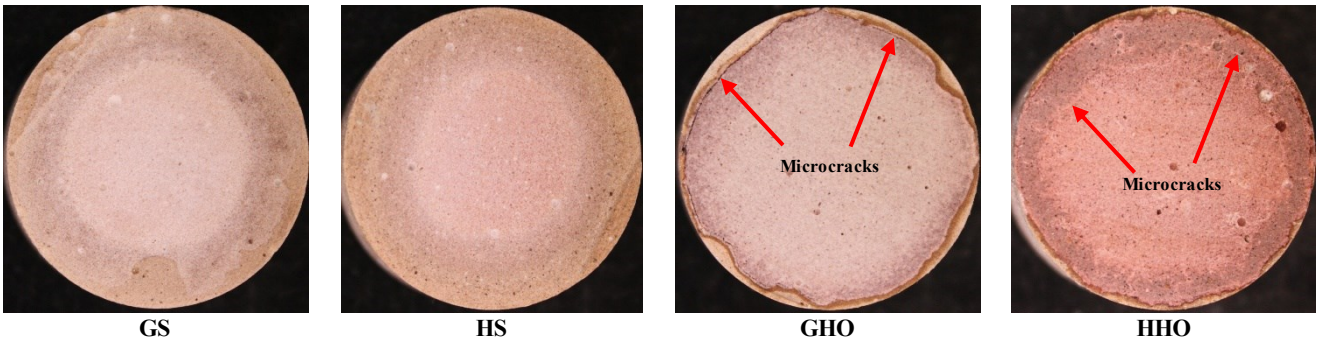

Fig. 8: Photos of aged cores after cross sectioning

4.3 Compressive Strength

Changes in the compressive strength of baseline samples have consistent with the occurrence of carbonation (**Fig. 9**). The baseline sample predominantly displayed increased compressive strength with a slight decrease in a few cases. Overall, Class H cement exhibited more carbonation than Class G cement. As a result, the average compressive strength increase for Class H cement was 92%, and that of Class G cement was 26%. Although the baseline samples demonstrated a temporary improvement in compressive strength, ultimately, their strength diminishes as the calcium carbonate crystals formed in the pore space react with carbonic acid and produce readily soluble calcium bicarbonate that the surrounding fluid can easily leach out.

HOAP samples exhibited a different compressive strengths behavior after aging. Except for one case (HHO samples in Experiment 7), they consistently showed a reduction in compressive strengths after aging, demonstrating the benefits of adding hydroxyapatite in preventing the carbonation of CH and CSH. On average, the decline was more pronounced in the case of GHO samples than HHO samples. While the reduction in strength is a main concern, the strength retained after the aging was still above the established industry standards. The decrease in strength could be associated with thermal retrogression CSH, which occurs due to the lack of silica flour in HOAP cement formulation. The strength reduction was minimal when the experiment was conducted at a low temperature (Experiment 5). HHO samples in Experiment 7 displayed a slight increase in compressive strength. One possible explanation for the strength increase could be the carbonation of calcium hydroxyapatite, which produces carbonated-hydroxyapatite that forms crystals in the pore space. The formation of the crystals with limited solubility can cause a moderate increase in compressive strength. The solubility of CO_2 is maximum under the conditions of Experiment 7.

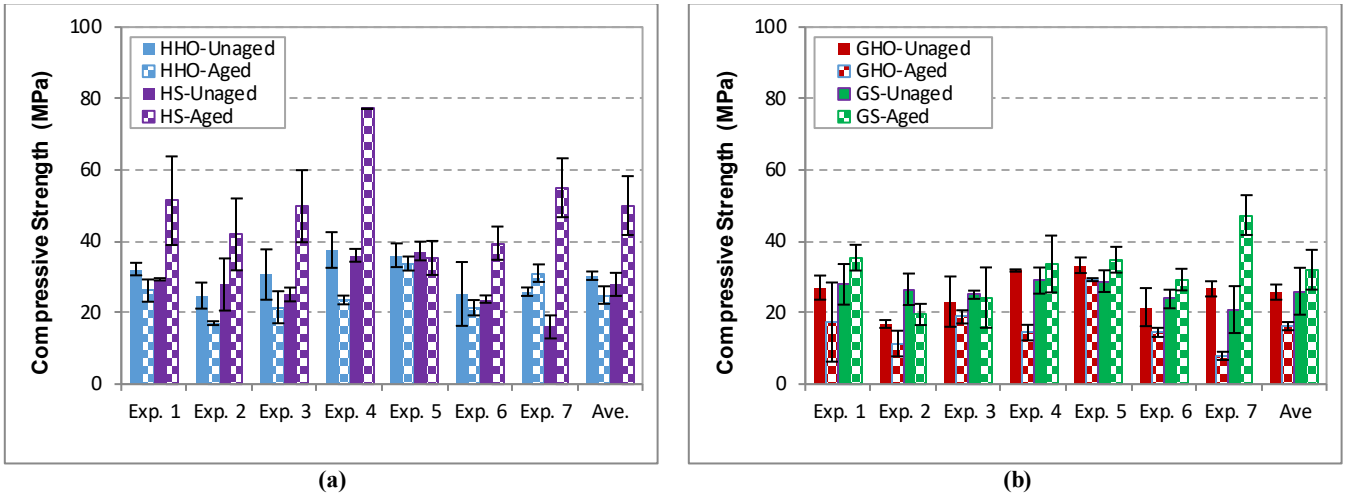

Fig. 9: Compressive strength of HOAP and baseline samples: a) HHO and HS, and b) GHO and GS

4.4 Shear Bond Strength

The shear bond strength (SBS) is the shear stress required to break the bond between cement and casing or cement and the wellbore. It is a major factor in determining the integrity of the wellbore. Only Class H cement (with and without hydroxyapatite) was used for SBS investigation. Carbonation consistently increased the SBS of HS samples (**Fig. 10**). The SBS of the sample increased due to the formation of calcium carbonate crystals in the pore space during the carbonation process. However, the SBS of HHO samples displayed a mixed trend of SBS after aging. The majority of the experiments showed a minor reduction in SBS after aging. The decrease was substantial for Experiment 7, conducted at extreme conditions (221°C, 100% CO_2, and 63 MPa). Permeability measurements and visual examination of the cores agree with this observation that can be explained by considering thermal retrogression. The unexpected rise in SBS displayed in Experiments 4 and 5 is inconsistent with compressive strength data. The solubility of CO_2 is expected to be high (Fig. 2) for this test condition. The increased CO_2 solubility causes more carbonation. Recent dental studies (Mao et al. 2009; Seah 2009) reported the improvement of the interfacial bond between implants and bones because of the carbonation of hydroxyapatite. Therefore, the unexpected rise in SBS could be due to the formation of carbonated hydroxyapatite.

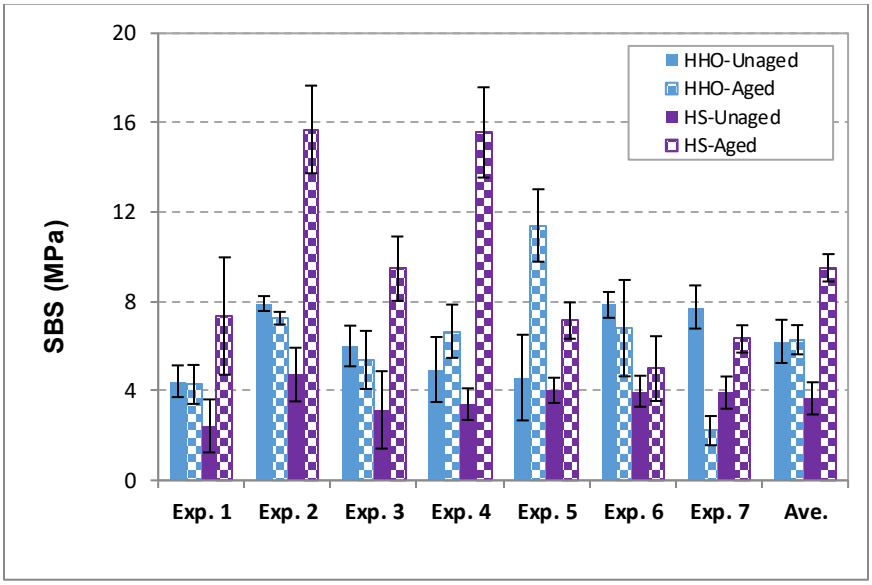

Fig. 10: Compressive strength of HOAP and baseline samples: a) HHO and HS, and b) GHO and GS

4.4 Mineralogical Composition

Three samples taken from different zones (outer, middle, and inner parts of the core) of transversely-cut cores were analyzed using FTIR equipment. The analysis was to determine their mineralogical composition (CH, CSH, calcium carbonate) and assess the level of carbonation that occurred after aging. The FTIR spectra of samples taken from three different zones of HS and HHO cores aged at 430° C and 63 MPa (Experiment 7) are presented in **Figs. 11** and **12**, respectively. The presence of CH, CSH, and calcium carbonate in the zones of interest in different amounts demonstrated the carbonation process. The minerals under focus are the carbonation reaction reactants (CH and CSH) and products ($CaCO_3$). The FTIR spectrum peaks of these materials are described in **Table 4**. CSH exists in various phases that have different spectrum peaks. As a result, a shift in the FTIR spectrum peak of CSH is expected when thermal

retrogression occurs. The FTIR spectrum peaks of CH (Wave number of 3645 cm^{-1}) presented in Figs. 11 and 12 confirmed its absence in the outer zones of the cores, while its strong presence was detected in the other zones of the cores. The absence of CH in the outer zone indicates the presence of a carbonation front between the outer and middle zones that moves toward the center of the cores as the carbonation process continues. This explanation can be supported by looking at the FTIR spectrum peak of calcium carbonate, which is expected to be produced when CH is consumed. Accordingly, a strong presence of calcium carbonate was detected in the outer zones of the cores, indicating the occurrence of significant carbonation. However, in the middle zone, the HS core exhibited a moderate presence of calcium carbonate, while the HHO core showed a minor presence of calcium carbonate. Therefore, the difference in the level of calcium carbonate in the middle zone indicates the benefit of adding hydroxyapatite in slowing the carbonation process. Samples from both cores showed the minor presence of calcium carbonate in their inner zones, demonstrating the occurrence of limited carbonation.

Table 4: FTIR spectrum peaks for various minerals (Srivastava et al. 2019)

Mineral	Wave number (cm^{-1})
CH	3645 (Nasrazadani and Eureste 2008)
CSH (Tobermorite gel)	950 - 1100 (Berzina-Cimdina and Borodajenko 2012; Yu et al. 1999)
CSH (Xonotlite)	400 - 500 (Hartmann et al. 2015)
$CaCO_3$	~1460 (Baciu and Simizis 2007)

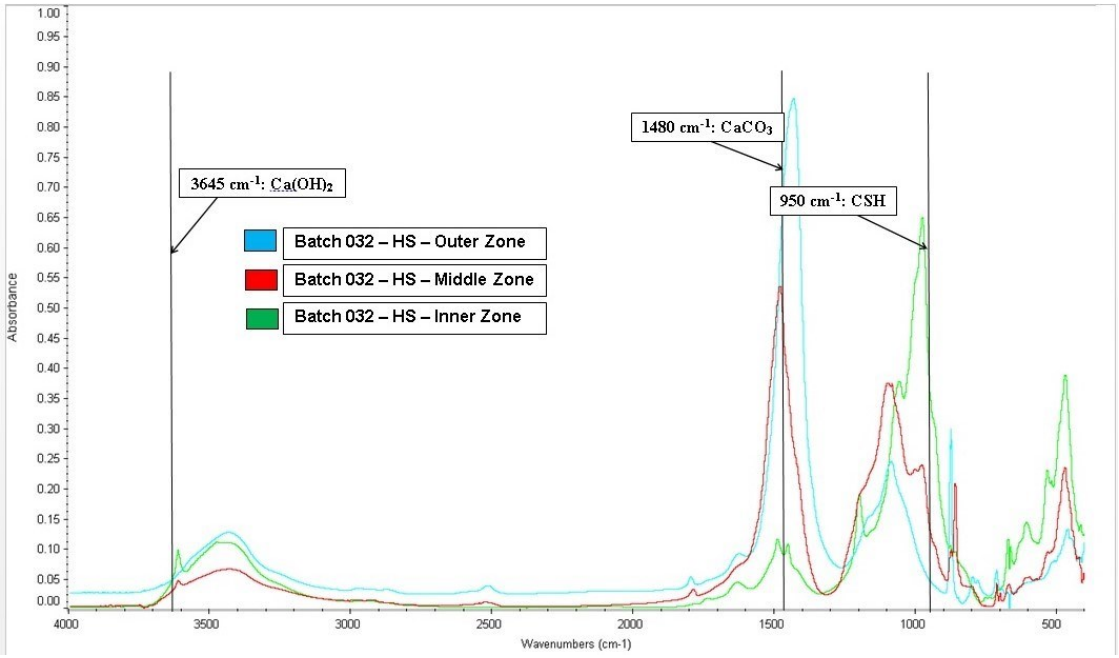

Fig. 11: FTIR spectra of samples taken from three different zones of HS core aged at 430° C and 63 MPa (Exp. 7)

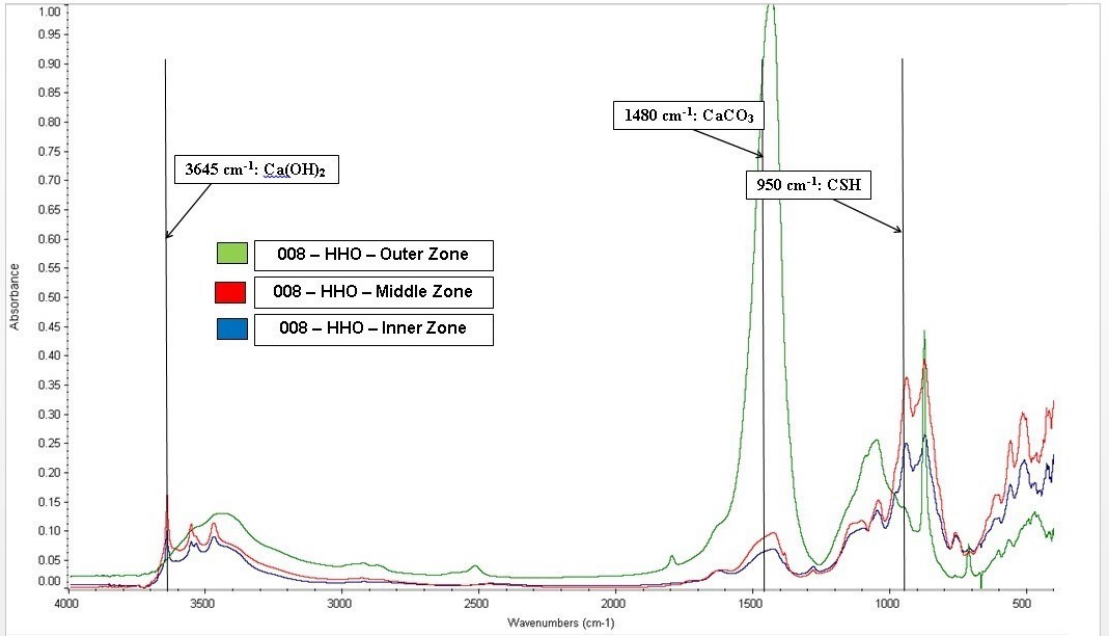

Fig. 12: FTIR spectra of samples taken from three different zones of HHO core aged at 430° C and 63 MPa (Exp. 7)

Even though the FTIR method is a powerful technique in determining the mineralogical composition of the substance, it can also give inconsistent results. The inconsistency often occurs when different minerals with similar chemical bonds are present in the material or the material contains a mineral that exhibits a wide range of spectrum peaks. The inconsistency occurs because the FTIR method directly detects the presence of a specific chemical bond, not directly the mineral. For instance, the -CO_3 bond peak present in the calcium carbonate spectrum also includes the -CO_3 bond of carbonated-hydroxyapatite. As a result, the FTIR method sometimes provides inconsistent results when a comparison is performed by looking at the spectrum peaks of the -CO_3 bond. Moreover, due to the existence of various phases, CSH exhibits a wide range of spectrum peaks that may cause inconsistency in carbonation analysis. Therefore, the spectrum peaks of CSH and calcium carbonate are excluded, and that of CH is used to evaluate the carbonation process.

For carbonation assessment, the FTIR spectrum of CH is simplified by determining the absorbance peak ratio (APR), which compares the quantity of a mineral present in different samples. The highest absorbance peak (Amax) is taken as 100, and other peaks are calculated based on their absorbance peak strength (A) as:

$$\text{APR} = \frac{A}{A_{Max}} \times 100. \tag{8}$$

It is important to note that the APR only compares the amount of a mineral present in HS and HHO samples; it doesn't represent the concentration of the mineral. **Figure 13** presents the average APR of CH in HHO and HS cores aged at different conditions. The average is determined from the APRs obtained from the cores' inner, middle, and outer zones. Results indicate the presence of more CH in HHO cores than HS cores, demonstrating hydroxyapatite's performance in reducing the carbonation of CH. Usually, CH is more reactive to carbonic acid than CSH (Fig. 3). Therefore, the preservation of CH indirectly means the conservation of CSH. The levels of CH in HHO and HS cores were comparable in two cases (Experiments 5 and 7), in which the experiments were conducted at high partial pressures of CO_2, and then solubility of CO_2 is expected to be high (Fig. 2).

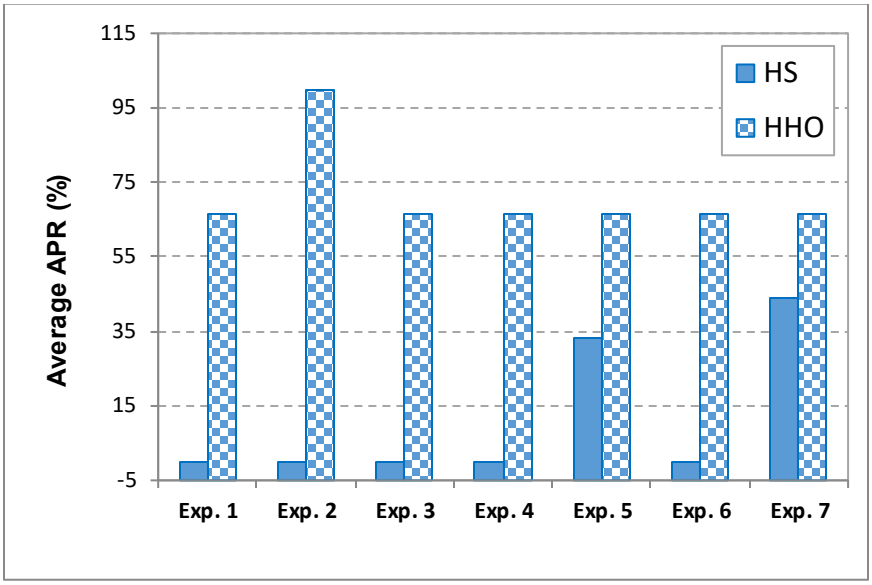

Fig. 13: Average APR of CH in HHO and HS cores aged at different conditions

5. CONCLUSIONS

In this study, hydroxyapatite is used to improve the carbonic acid resistance of Class H and Class G cements. Hence, cement formulations (HOAP) that contain 5% hydroxyapatite were developed. For evaluating the new formulations' carbonic acid resistance, aging experiments were conducted with baseline (HS and GS) and new HOAP (HHO and GHO) cement samples. Then, the properties of aged and unaged cement samples of each formulation were measured and compared. Based on the outcomes of this study, the following conclusions can be made:

- Hydroxyapatite can be used as an additive to create Class H and Class G cement slurry formulations that can satisfy the slurry property requirements established for zonal isolation of HPHT Wells.
- For temperatures ranging from 38 to 177°C, the addition of 5% hydroxyapatite remarkably enhanced the resistance of Class H and Class G cements against carbonic acid. The presence of a more significant amount of CH in HHO than HS cement after exposure to carbonic acid demonstrated the reduction of carbonation.
- After aging in harsh environments containing carbonic acid, the HOAP samples predominantly retained their original properties while the baseline samples exhibited considerable property change.
- Due to thermal retrogression and subsequently cracking, HOAP cement lost its sealing performance when exposed to extremely high temperatures (greater than 221°C). Hence, the incorporation of silica flour is crucial for the applicability of hydroxyapatite-based cement in high-temperature well applications. For incorporating silica flour, more effective dispersants and retarders must be utilized to control the slurry viscosity and thickening time.

ACKNOWLEDGMENT

The authors acknowledge the Bureau of Safety and Environmental Enforcement (BSEE) for sponsoring this project (E12PC00035) and the University of Oklahoma for providing the necessary project support.

NOMENCLATURE

Symbols

K_{sp}	Total solubility product
K_{sp}^{Cl}	Solubility product due to chlorine ion concentration
K_{sp}^{T}	Solubility product due to temperature effect
T	Temperature
X_{NaCl}	Concentration of NaCl in water

Acronyms

API	American Petroleum Industry
ASTM	American Society for Testing and Materials
BWOC	by Weight of Cement
CH	Calcium Hydroxide
CSH	Calcium Silicate Hydrate
DAQ	Data Acquisition
FTIR	Fourier Transform Infra-Red
HEC	HydroxylEthylCellulose
HHO	Class H cement containing 5% hydroxyapatite by weight of cement
HPHT	High-pressure High-temperature
HS	Class H cement containing silica flour
SBS	Shear Bond Strength

REFERENCES

Ahmed, R., Shah, S., Osisanya, S., Hassani, S., Elgaddafi, R., Maheshwari, H. and Naidu, A. 2012. Effect of H2S and CO2 in HPHT Wells on Tubulars and Cement, Monthly Report# 10, BSEE Project# E12PC00035, University of Oklahoma.

Bassett, H. 1934. Notes on the system lime-water, and the determination of calcium. J. Chem. Soc., pp. 1270-1275, 10.1039/JR9340001270.

Benge, G. 2009. Improving well bore seal integrity in CO2 injection wells. Energy Procedia, Vol. 1, 3253-3529.

Berzina-Cimdina, L. and Borodajenko, N. 2012. Research of Calcium Phosphate Using Fourier Transform Infrared Spectroscopy, Chapter 6-Infrared Spectroscopy - Materials Science, Engineering and Technology, Intech, Croatia.

Bjørge, R., Gawel, K. , Panduro, E. A. C. and Torsæter, M. 2019. Carbonation of silica cement at high-temperature well conditions, International Journal of Greenhouse Gas Control 82, 261–268.

Brandl, A., Cutler, J., Seholm, A., Sansil, M. and Braun, G. 2010. Cementing Solutions for Corrosive Well Environments. Paper SPE 132228-MS presented at International Oil & Gas Conference and Exhibition, China, 8-10 June. http://dx.doi.org/10.2118/132228-MS.

Dillenbeck, III R. L., Mueller D. T., and Orr B. R. 1990. The Effect of MicroSilica on the Thermal Stability of Lightweight Cement Systems, Paper SPE-21597 presented as the CIM/SPE International Technical Meeting, 10-13 June, Calgary, Canada.

Duan, Z., and Sun, R. 2003. An improved model calculating CO2 solubility in pure water and aqueous NaCl solutions from 257 to 533 K and from 0 to 2000 bar. Chem. Geol. 193, 257–271.

Duguid, A. 2009. An estimate of the time to degrade the cement sheath in a well exposed to carbonated brine. Energy Procedia Vol. 1, 3181-3188.

Eilers, L. H. and Root R. L. 1976. Long-Term Effects of High Temperature on Strength Retrogression of Cements, Paper SPE 5871 presented at the SPE California Regional Meeting, 7-9 April, Long Beach, California.

Eilers L. H., Nelson E. B. and Moran L. K. 1983. High Temperature Cement Compositions – Pectolite, Scawtite, Truscotite or Xonoloite: Which Do You Want? JPT-0149-2136/83/0007-9286 (July).

Gerard, B. Le Bellego, C. and Bernard, O. 2002. Simplified modeling of calcium leaching of concrete in various environments. Materials and Structure, Vol. 35, 632-640.

Glasser, F.P., Pedersen, J., Goldthorpe, K. and Atkins, M. 2005. Solubility reactions of cement components with NaCl solutions: I. Ca(OH)2 and C-S-H. Adv. Cem. Res., 17, pp. 57-64, 10.1680/adcr.2005.17.2.57.

Glasser, F.P. and Matschei, T. 2007. Interactions between Portland Cement and Carbon Dioxide. 12th international Congress on the chemistry of cement, Montréal Canada, 8 - 13 July.

Grabowski, E. and Gillott J. E. 1989. Effect of Replacement of Silica Flour with Silica Fume on Engineering Properties of Oil Well Cements at Normal and Elevated Temperatures and Pressures, Cement and Concrete Research 19, 333-344.

Hwang, J., Ahmed, R.M., Tale, S. and Shah, S. 2018. Shear bond strength of oil well cement in carbonic acid environment, Journal of CO2 Utilization, Vol. 27, 60-72.

Lea, F. M. 1971. The Chemistry of Cement and Concrete, Third Edition, Chemical Publishing Company, 841-905.

Loo, Y., Chin, M., Tam, C. and Ong, K. 1994. A carbonation prediction model for accelerated carbonation testing of concrete. Mag. Concr. Res., 46, pp. 191-200.

Krilov, Z., Loncaric, B. and Miksa, Z. 2000. Investigation of a Long-Term Cement Deterioration under a High-Temperature, Sour Gas Down-hole Environment. Paper SPE 58771 presented at SPE International Symposium on Formation Damage Control, Lafayette, Louisiana, 23-24 February.

Kutchko, B., Stratzisar, B., Dzombak, D.A. Lowry, G.V. and Thaulow, N. 2007. Degradation of well cement by CO2 under geologic sequestration conditions. Environ. Sci. Technol. Vol. 41, 4787-4792.

Mao, K., Yang, Y., Li, J., Hao, L., Tang, P., Wang, Z., Wen, N., Du, M., Wang, J. and Wang, Y. 2009. Investigation of the histology and interfacial bonding between carbonated hydroxyapatite cement and bone, Biomedical Materials, IOP Publishing Ltd, 17 June.

Martin, R.I. and Brown, P.W. 1995. Mechanical properties of Hydroxyapatite formed at physiological temperature, Journal of Material Science: Materials in Medicine 6, 138-143.

Matsuzawa, K., Kitsutaka, Y. and Tsukagoshi, M. 2010. Effect of humidity on rate of carbonation of concrete exposed to high-temperature environment. 4th Int. Symp. Ageing Manag. Maint. Nucl. Power Plants (ISaG 2010), Mitsubishi Research Institute, University of Tokyo, Japan, pp. 109-114.

Nakarai, K., Ishida, T. and Maekawa, K. 2006. Modeling of Calcium Leaching from Cement Hydrates Coupled with Micro-pore Formation. Journal of Advanced Concrete Technology 4 (3), 395-407.

Nasrazadani, S. and Eureste, E. 2008. Application of FTIR for Quantitative Lime Analysis, University of North Texas, Report No. 5-9028-01-1, April.

Omosebi, O., Maheshwari, H., Ahmed, R. M., Shah, S. N., Osisanya, S. 2017. Experimental study of the effects of CO2 concentration and pressure at elevated temperature on the mechanical integrity of oil and gas well cement. Journal of Natural Gas Science and Engineering, 44, 299-313.

Omosebi, O., Maheshwari, H., Ahmed, R. M., Shah, S. N., Osisanya, S., Hassani, S., DeBruijn, G., Cornell, W. and Simon, D. 2016. Degradation of well cement in HPHT acidic environment: Effects of CO2 concentration and pressure, Cement and Concrete Composites 74, November, DOI: 10.1016/j.cemconcomp.2016.09.006.

Omosebi, O., Maheshwari, H., Ahmed, R. M., Shah, S. N., Osisanya, S., Santra, A., Saasen, A. 2015. Investigating temperature effect on degradation of well cement in HPHT carbonic acid environment. Journal of Natural Gas Science and Engineering 26, 1344–1362.

Papadakis, V.G., Vayenas, C.G. and Fardis, M.N. 1991. Fundamental modeling and experimental investigation of concrete carbonation. ACI Mater. J., 88, pp. 363-373.

RP10B, 1997. API Recommended Practice for Testing Well Cements, 1 December.

Samson, E. and Marchand, J. 2007. Modeling the effect of temperature on ionic transport in cementitious materials. Cement and Concrete Research, Volume 37, Issue 3, Pages 455-468, https://doi.org/10.1016/j.cemconres.2006.11.008.

Santra, A. and Sweatman, R. 2011.Understanding the Long-Term Chemical and Mechanical Integrity of Cement in a CCS Environment. Energy Procedia, Vol. 4, 5243-5250.

Šavija, B. and Luković, M. 2016. Carbonation of cement paste: Understanding, challenges, and opportunities, Construction and Building Materials, Volume 117, 1 August 2016, Pages 285-301.

Seah, R. K. H., Garland, M., Loo, J. S. C. and Widjaja, E. 2009. Use of Raman Microscopy and Multivariate Data Analysis to Observe the Biomimetic Growth of Carbonated Hydroxyapatite on Bioactive Glass, Anal. Chem., 81, 4, 1442-1449.

Srivastava, A. 2014. Effects of Additives on Oil Well Cement Under HPHT Acidic Environment. Master of Science thesis, University of Oklahoma.

Srivastava, A., Ahmed, R. and Shah, S. 2019. Carbonic Acid Resistance of Hydroxyapatite Based Cement. Paper SPE-193585-PA, SPE Drilling & Completion, Vol. 35, July, https://doi.org/10.2118/193585-PA.

Sugama, T. and Carciello, N. R. 1992. Carbonation of Hydrothermally Treated Phosphate-Bonded Calcium Aluminate Cements, Cement and Concrete Research 22, 783-792.

Sugama, T. and Carciello, N. R. 1993. Carbonation of Calcium Phosphate Cements after Long Term Exposure to Na2CO3-Laden Water at 250°C. Cement and Concrete Research 23, 1409-1417.

Sugama, T. 2006. Advanced Cements for Geothermal Wells. Final Report for the US Department of Energy Office of Geothermal Technologies, July.

Taylor, H. F. W., 1964. The chemistry of cements. Academic Press, London.

Teraoka, K., Ito, A., Maekawa, K., Onuma, K., Tateishi T. and Tsutsumi, S. 1998. Mechanical Properties of Hydroxyapatite and OH-Carbonated Hydroxyapatite Single Crystals. Journal of Dental Research 77 (7), 1560-1568.

Yu, P., Kirkpatrick, R.J., Poe, B., McMillan, P.F. and Cong, X. 1999. Structure of Calcium Silicate Hydrate (C-S-H): Near-, Mid-, and Far-Infrared Spectroscopy, J. Am. Ceram. Soc., 82 [3] 742–48.